Combining Experiments and Simulation of Gas Absorption for Teaching Mass Transfer Fundamentals: REMOVING CO_2 FROM AIR USING WATER AND NAOH

WILLIAM M. CLARK, YAMINAH Z. JACKSON, MICHAEL T. MORIN, AND GIACOMO P. FERRARO
Worcester Polytechnic Institute, Worcester MA 01609

One educational goal of the unit operations laboratory is to help students understand fundamental principles by connecting theory and equations in their textbooks to real-world applications. We have found, however, that collecting data and analyzing it with empirical correlations does not always translate into a good understanding of what is happening inside the pipes.[1] One problem is that the theoretical development behind the labs is often comprised of approximate methods using lumped parameters that describe the results but not the details of the physical process. For example, when a mass transfer coefficient is obtained from an absorption experiment, some students struggle to explain what the mass transfer coefficient represents and why it increases with increasing absorbent flow rate. To address this problem, we are using computer simulations to solidify the link between experiment and theory and provide improved learning.[1,2]

Commercial software packages like COMSOL Multiphysics™ allow students to set up and solve the partial differential equations that describe momentum, energy, and mass balances and also to visualize the velocity, pressure, temperature, and concentration profiles within the equipment. Visualization of the processes may not only help reinforce concepts and clarify the underlying physics but it may also help "bring to life" the mathematics as well as the experiments. With this software, students don't necessarily need to know the details of how to solve complex equations, but they need to know which equations to solve and how to validate the results.[3] This type of simulation can also extend the range of experience beyond what is possible in the lab by allowing studies that would otherwise be prohibited by time, financial, or safety constraints.

In this paper we present experiments and computer models for studying the environmentally important problem of removing CO_2 from air. Simple models are shown to provide straightforward analysis of the experimental data even when the system is not dilute. In addition, we present more detailed models that illustrate the two-film theory and provide insight

William Clark *is an associate professor of chemical engineering at Worcester Polytechnic Institute. He received a B.S. degree from Clemson University and a Ph.D. degree from Rice University, both in chemical engineering. He has more than 20 years of experience teaching thermodynamics and unit operations laboratory at WPI. In addition to research efforts in teaching and learning, he has conducted disciplinary research in separation processes.*

Yaminah Jackson *graduated from the WPI Chemical Engineering Department in Spring 2008. She is currently attending graduate school at the University of Southern California.*

Michael Morin *graduated from the WPI Chemical Engineering Department in Spring 2009. He is currently a Ph.D. candidate in mechanical engineering at WPI.*

Giacomo Ferraro *is the laboratory manager in the Chemical Engineering Department at WPI. He is a master machinist and has facilitated equipment design, fabrication, and use for teaching and research at WPI for more than 30 years.*

into the absorption process. These models help explain the absorbent flow rate dependence of the mass transfer coefficient and how the process is liquid phase resistance controlled when using water and dependent on the gas phase resistance when using dilute NaOH solution as absorbent. Finally, we provide some discussion of how the simulations have been received by students.

LABORATORY EXPERIMENT

A few years ago our old 30-foot-tall, 6-inch-diameter, steel absorption tower became clogged with rust and residue from years of use with sodium carbonate solution as absorbent for removing CO_2 from air. Since concerns over global warming are a political reality even if the causes and effects are not clear, we wanted to continue to offer a CO_2 absorption experiment because of its appeal to student interest as well as its ability to illustrate mass transfer fundamentals. To reduce cost and avoid column fouling in the future, we chose to use pure water as absorbent in our new 6-foot-tall, 3-inch-diameter, glass column packed with 54 inches of ¼-inch glass Raschig rings that we purchased from Hampden Engineering Corporation[4] and modified to suit our needs. Although using water as absorbent focuses the lab on mass transfer concepts without the added complexity of reactions, the limited solubility of CO_2 in water makes it necessary to have accurate analysis of the gas phase and to work with concentrated gas streams to get good results. A Rosemount Analytical, Inc.,[5] model 880a infrared analyzer provides accurate and reliable measurement of the CO_2 composition of the gas phase at the column entrance and exit. To measure a significant change in the gas phase composition, it is best if the gas rate is low and the water rate is high. Having a low gas rate also provides the benefit of consuming less CO_2 (and air) and emitting less CO_2 to the environment in both the exiting gas and water streams.

To illustrate the advantage of combining a chemical reaction with the absorption process, we also built a small-scale column for use with NaOH solution as absorbent. A 1.75-in-diameter, 15-in-long acrylic tube was filled to a height of 12.75 in with the same glass rings used in our larger column. End caps for the acrylic column were made with rubber stoppers fitted with liquid and gas inlet and outlets.

We describe here the analysis of representative sets of experimental runs using the two columns. Our students use the larger column to determine the effect of water flow rate on the mass transfer process. Experimental data are presented in Table 1 for four different water flow rates at fixed gas phase inlet conditions and room temperature. At present we don't have our students working with NaOH in the lab for safety reasons. Instead, we give them data obtained on the smaller column by a student working on his senior thesis. Table 2 shows the data collected for both water and 1 N NaOH solution at five different liquid rates and a fixed gas phase inlet condition at room temperature. It can be seen that very little CO_2 is removed in the small column at these conditions with water as absorbent. On the other hand, most of the CO_2 is removed from the gas stream when NaOH is used, even in the small column.

TABLE 1
Large Column Data and Results for CO_2 Absorption from Air Using Water at Room Temperature
Air Rate, A = 1.42 L/min; Inlet CO_2, y_b = 0.185

Water Rate, W L/min	Outlet CO_2, y_t mole fraction	$K_y a$ mol/m³s
0.53	0.143	0.333
1.06	0.099	0.558
1.58	0.064	0.634
2.11	0.039	0.712

TABLE 2
Small Column Data and Results for CO_2 Absorption From Air Using Water or 1 N NaOH at Room Temperature
Air Rate, A = 1.5 L/min

	y_b = 0.175 (water)		y_b = 0.178 (NaOH)	
Liquid Rate, W L/min	Outlet CO_2, y_t mole fraction	$K_y a$ mol/m³s	Outlet CO_2, y_t mole fraction	$K_y a$ mol/m³s
0.14	0.168	0.237	0.062	2.96
0.23	0.165	0.285	0.050	3.69
0.28	0.164	0.312	0.037	4.09
0.35	0.162	0.349	0.031	4.66
0.40	0.161	0.375	0.027	5.07

TABLE 3
Heights of Transfer Units and Mass Transfer Coefficients for Large Column

Water Rate L/min	H_x m	H_y m	mGH_x/L m	H_{Oy} m	$k_y a$ mol/m³s	$k_x a$ mol/m³s	$k_x a/m$ mol/m³s	$K_y a$ correlated
0.53	0.193	0.065	0.591	0.656	3.55	557	0.392	0.353
1.06	0.238	0.046	0.363	0.410	5.02	904	0.637	0.565
1.58	0.268	0.038	0.275	0.313	6.13	1196	0.842	0.740
2.11	0.292	0.033	0.225	0.257	7.08	1464	1.031	0.900

TRADITIONAL ANALYSIS

If we neglect temperature and pressure effects and assume that CO_2 only is experiencing mass transfer between the gas and the liquid phases, traditional analysis leads to a design equation for our absorber given by[6]:

$$Z = \int_0^Z dz = \frac{G_0}{K_y a}\int_{y_b}^{y_t}\frac{dy}{(1-y)^2(y-y_e)} = H_{Oy}N_{Oy} \qquad (1)$$

where t and b represent top and bottom of the column, respectively, Z is the column height, y is the gas phase CO_2 mole fraction, y_e is the value of the gas phase CO_2 mole fraction that would be in equilibrium with the liquid phase, $K_y a$ is the overall mass transfer coefficient based on the gas phase driving force, G_0 is the solute free gas flux, H_{Oy} is called the height of a transfer unit, and N_{Oy} is the number of transfer units.

Neglecting details of reactions between CO_2 and water and any impurities we can describe the vapor liquid equilibrium with Henry's law using Henry's constant, H = 1420 atm at 20 °C.[7] Since the height of the laboratory column is known, experimental gas phase composition data can be used in Eq. (1) to solve for the mass transfer coefficient at various operating conditions.

Integrating Eq. (1) is tedious since a mass balance in the form of an operating line equation must first be used to determine x at every value of y before Henry's law can be used to find y_e at each x that corresponds to each y. This has traditionally been done by plotting the operating line and the equilibrium line and then graphically integrating Eq. (1). Modern computing environments like MATLAB™ can be used to integrate this equation and back out mass transfer coefficients from laboratory data as shown in Appendix 1. Results for $K_y a$ obtained by this method are given in Table 1 and these can be seen to increase with increasing water rate.

The traditional analysis doesn't give much insight into the details of the mass transfer process or the physical reason the mass transfer improves with increasing water rate. To obtain that insight, students are directed to textbooks for an explanation of the two-film theory of Whitman[8] where they learn that the overall resistance to mass transfer can be considered to be made of a gas phase film resistance and a liquid phase film resistance:

$$H_{Oy} = H_y + m\frac{G}{L}H_x \qquad (2)$$

or equivalently,

$$\frac{1}{K_y a} = \frac{1}{k_y a} + \frac{m}{k_x a} \qquad (3)$$

where m is the slope of the equilibrium line, equal to the Henry's constant here. Geankoplis[7] gives correlations for H_x and H_y and the results of these correlations are given in Table 3.

A few years ago our old 30-foot-tall, 6-inch-diameter, steel absorption tower became clogged with rust and residue from years of use with sodium carbonate solution as absorbent for removing CO_2 from air.

Although these correlations are not generally expected to give accurate quantitative predictions, the correlated results for $K_y a$ are in reasonably good agreement with the experimentally obtained results.

H_{Oy}, H_x, and H_y are often thought of as the overall, liquid side, and gas side resistance to mass transfer, respectively. Confusion can result, however, when using these to explain the water rate dependence of the mass transfer coefficient, because while H_x is larger than H_y, H_x is observed to increase rather than decrease with increasing water rate. Apparently the term mGH_x/L is the controlling factor here, but this still doesn't provide a clear physical explanation.

SIMPLE MODEL

Our simple absorber model uses COMSOL Multiphysics to solve two instances of the convection and diffusion equation simultaneously with appropriate boundary conditions in a cylinder with the dimensions of our column:

$$\nabla\cdot(-D\nabla c) = R - \vec{u}\cdot\nabla c \qquad (4)$$

R represents a reaction or source term and $\vec{u}$ is the velocity vector in the convection term. One instance of Eq. (4) evaluates the concentration of solute in the gas phase, c_g, and the other instance evaluates the concentration of solute in the liquid phase, c_l. In the simple model, we included a mass transfer term as a "reaction" and consider that solute leaving the gas phase by this "reaction" enters the liquid phase by a similar mass transfer "reaction." For the gas phase, the mass transfer "reaction" was written as

$$R = -K_y a(1-y)(y-y_e) \qquad (5)$$

The quantity (1-y) accounts for part of the $(1-y)^2$ term in Eq. (1) while the other part is accounted for by setting the gas velocity in the z-direction to $v_g = v_{g0} / (1-y)$. Thus, the changing gas velocity along the length of the column is easily taken into account. This treatment was not needed for the liquid phase because the small amount of solute dissolved in the liquid had a negligible effect on the liquid velocity.

The absorber can be modeled equally well in 1-D, 2-D, or 3-D, but we prefer the 2-D axial symmetric implementa-

tion because it gives the best visual representation of our process. One of the important advantages of the powerful modern computing environments is that there is usually no need for transformation or scaling of variables; we can work with the actual dimensions of the equipment and with SI dimensioned variables. This what-you-see-is-what-you-get philosophy is aimed at making a strong connection between the equations and the physical process and appealing to visual learners.

The model results can be presented in a variety of ways including a colorful surface plot of y within the column geometry (not shown here) and plots of y and x vs. column height as shown in Figure 1. As an example of the wealth of information readily obtained from the model, it is of interest to note that only three of the four experimentally obtained $K_y a$ results in Table 1 follow the expected trend of a linear function of water rate raised to the 0.7 power.[6] At first, we rationalized that the reason the first point, at the lowest water rate, did not follow the expected trend may have been channeling or poor wetting of the packing at this water rate. When we observed the liquid phase mole fraction, x, as a function of column height in our model for this run, however, we saw that the liquid was essentially saturated before reaching the column outlet. Thus, the experimental outlet results can be modeled using a wide range of $K_y a$ values including the value of 0.333 mol/m^{3}s that we obtained earlier but also the value of 0.480 mol/m^{3}s that would fall in line with our other results in a correlation of $K_y a$ vs. $(W)^{0.7}$.

Here we have used our model to calculate the outlet concentrations that will occur in the column given an overall mass transfer coefficient. We could just as easily have used the built-in Parametric Solver capability of COMSOL to find the values of the mass transfer coefficients that fit our experimental data. Our model could be easily modified to include variable mass transfer coefficients, multiple solutes, temperature and pressure effects, and even time dependence, but these modifications were not needed here. We have included the effect of the chemical reaction between NaOH and CO_2, however.

MODEL WITH REACTION

The chemical reaction between CO_2 and NaOH is well studied and according to the literature[10] the rate limiting step in this reaction is:

$$CO_2 + OH^- \rightarrow HCO_3^- \tag{6}$$

and the rate of reaction can be expressed as:

$$r = k_B C_{CO2} C_{OH^-} \tag{7}$$

with second order rate constant given as a function of ionic strength by

$$\log\left(k_B\right) = 11.875 - 2382 / T + 0.221\, I - 0.016\, I^2 \tag{8}$$

where k_B is in m^3/kmol s, T is in K, and I is in kmol/m^3. The ionic strength is calculated as

$$I = 0.5\left(C_{Na^+} + C_{OH^-} + 4\, C_{HCO3^-}\right) \tag{9}$$

Our absorber model was easily modified to account for this chemical reaction by writing the "reaction" term for CO_2 in the liquid phase as

$$R = K_y a\left(y - y_e\right) - k_B C_{CO2}\, C_{OH^-} \tag{10}$$

indicating that CO_2 arrives at the liquid phase from the gas phase by mass transfer and disappears from the liquid phase by reaction. This model also keeps track of the ions, Na^+, OH^-, and HCO_3^-, by solving Eq. (4) for each species in the liquid phase.

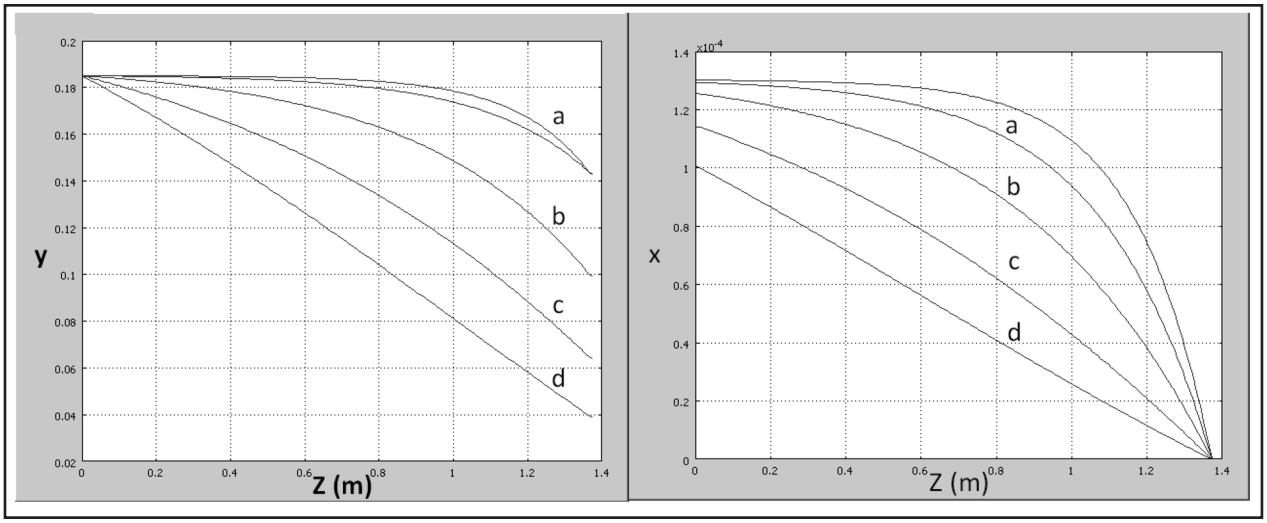

***Figure 1**. Mole fraction CO_2 in the gas and liquid phases as a function of column height at four different water rates: (a) W = 0.53 L / min, (b) W = 1.06 L/min, (c) W = 1.58 L/min, and (d) W = 2.11 L/min. Upper (a) curve is for $K_y a$ = 0.480, lower (a) curve is for $K_y a$ = 0.333 mol/m^{3}s.*

The Parametric Solver in COMSOL was used to find the values of $K_y a$ needed to make the outlet y results of the model match the experimental y results. The resulting $K_y a$ values are shown in Table 2. The dramatic improvement in the mass transfer process due to the reaction is reflected in the increase in $K_y a$ with reaction compared to without.

QUALITATIVE FALLING FILM MODEL

Although our simple absorber model is easier to use than the traditional analysis and has the added benefit of showing a colorful representation of the composition in the column, it doesn't given much insight into the details of the process or help explain why the mass transfer coefficients increase with increasing water flow rate. The physical process that actually occurs inside the column is that solute diffuses through a flowing gas phase to the gas-liquid interface, crosses the interface to maintain equilibrium there, and diffuses into a flowing liquid phase. To model this process more directly we should solve Eq. (4) with R = 0 and use the actual diffusion coefficients in the gas and liquid phases and an appropriate boundary condition at the interface. We describe here a qualitative diffusion-based falling film model aimed at addressing these concerns and providing a basis for understanding an explicit two-film model presented below.

Inside our packed column are glass rings that have a thin layer of water flowing down over them surrounded by gas flowing upward. Although it can be done, it is complicated and expensive in computer time to model the exact details of the fluid flow and mass transfer that takes place around these rings randomly packed inside the column. As an illustration, however, it was reasonable to approximate the process with a number of identical glass rods each extending the full height of the column. The water layer around each rod was considered to flow downward in laminar flow and the gas layer around that was considered to flow upward in plug flow. The thickness and velocities in these flowing layers were selected to give approximate results that illustrate our points. It was only necessary to model one rod with its surrounding layers axially symmetrically as shown in Figure 2.

As before, two instances of the convection and diffusion equation, one for the gas phase and one for the liquid phase, were solved simultaneously. The inlet and outlet boundary conditions are shown in Figure 2. The so-called "stiff-spring" equilibrium boundary condition[11] was used at the gas-liquid interface according to Henry's law. That is, the boundary condition on the gas side of the interface was set to

$$\text{Flux} = -M\left(y - y_e\right) \tag{11}$$

and the boundary condition on the liquid side was set to

$$\text{Flux} = M\left(y - y_e\right) \tag{12}$$

where M is an arbitrary large number; *e.g.*, M = 10000. This assures a continuous flux across the interface and enforces the equilibrium condition $y_e = H\,x$. Mass transfer coefficients were not used in this diffusion-based model. Instead, carbon dioxide diffuses through the gas phase, crosses the interface, and diffuses into the liquid phase according to molecular diffusion using diffusivities for CO_2 in air and water of 1.6×10^{-5} m^2/s and 1.8×10^{-9} m^2/s, respectively. The velocity profile in the liquid phase was given by the solution to the built-in Incompressible Navier-Stokes mode of COMSOL. The velocity in the gas phase was considered uniform in the r-direction but decreased as v_{g0} / (1-y) in the z-direction.

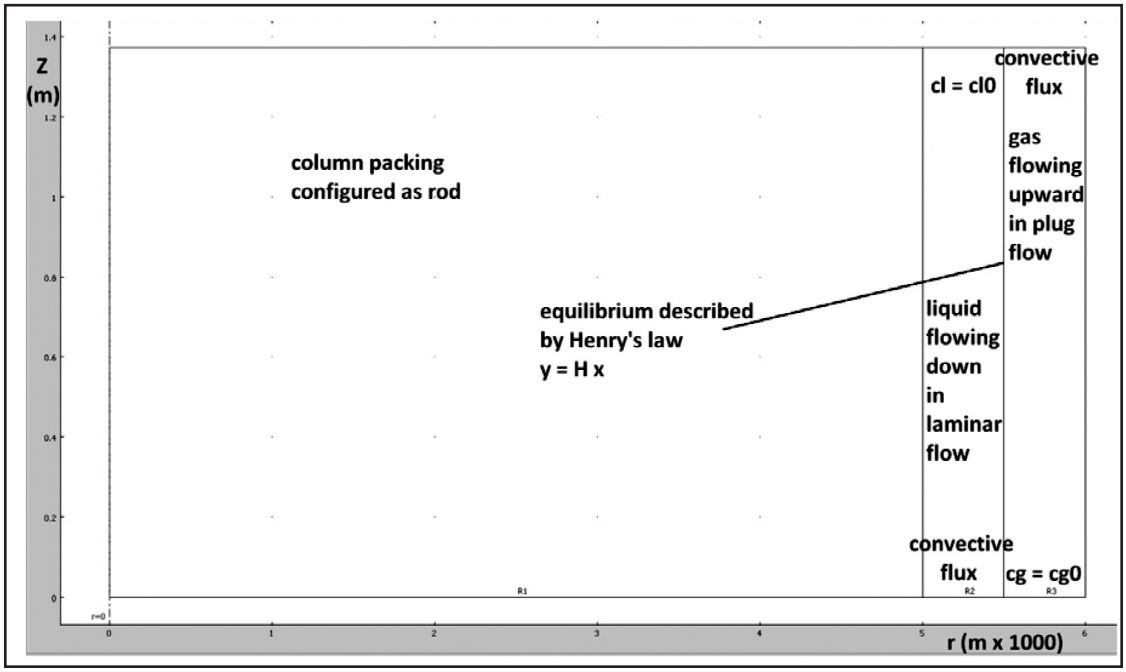

Figure 2. *Falling film model geometry.*

Figure 3 shows the resulting CO_2 concentration profile in the r-direction at a height equal to Z/10 for two different water velocities. Curve a is for a relatively low water rate and the curve b is for a relatively high one. More CO_2 is removed from the gas phase at the high water rate as expected. In both cases, the gas phase concentration is nearly uniform in the r-direction. On the other hand, the liquid phase concentration varies in the r-direction and can be characterized as having a rapidly changing region close to the interface and a nearly constant region in the bulk. The region where the concentration changes is often called the concentration boundary layer.[12] Figure 3 shows that the thickness of this boundary layer decreases with increasing water rate due to increased convection. In reality, a change in water rate would probably affect the interfacial area as well as the boundary layer thickness, but we have chosen to illustrate the process with a constant interfacial area.

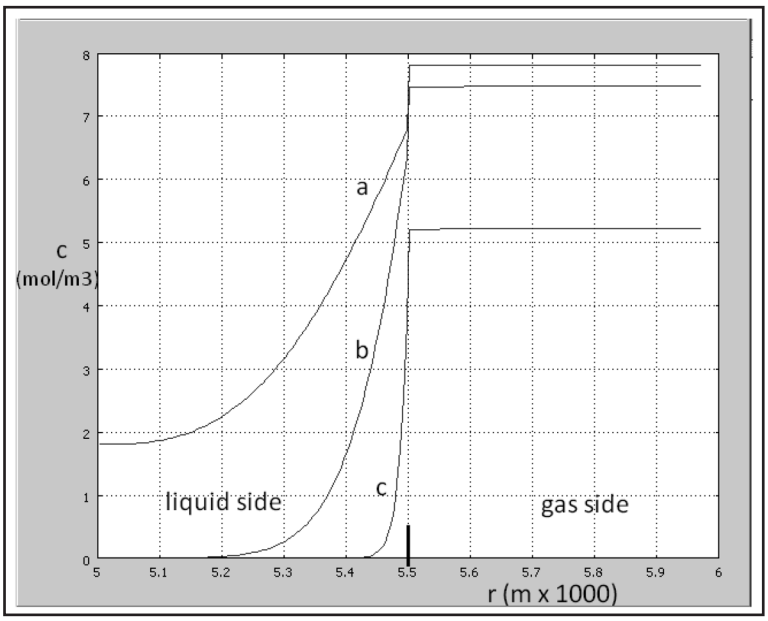

Figure 3. *Concentration in the r-direction at z/Z = 0.1 for qualitative falling film model (a) low water rate, (b) high water rate, (c) NaOH solution rate equal to water rate in (a). Note that the x-axis begins at r = 0.005 m to show only the flowing layers in this figure.*

Our qualitative falling film model was also modified to account for the chemical reaction. In this case, R in the liquid phase was given by Eq. (7). The resulting CO_2 concentration profile shown in Figure 3c indicates that the thickness of the concentration boundary layer over which the concentration is changing is greatly reduced when the reaction is present in the liquid phase.

EXPLICIT TWO-FILM MODEL

Our falling film model illustrates the diffusion and convection process but does not give accurate predictions for outlet compositions because it does not take into account all the details of the non-uniform packing and flow patterns in the column. We describe here an explicit two-film model that gives accurate outlet compositions, illustrates the two-film theory, and provides a physical interpretation of the mass transfer coefficient.

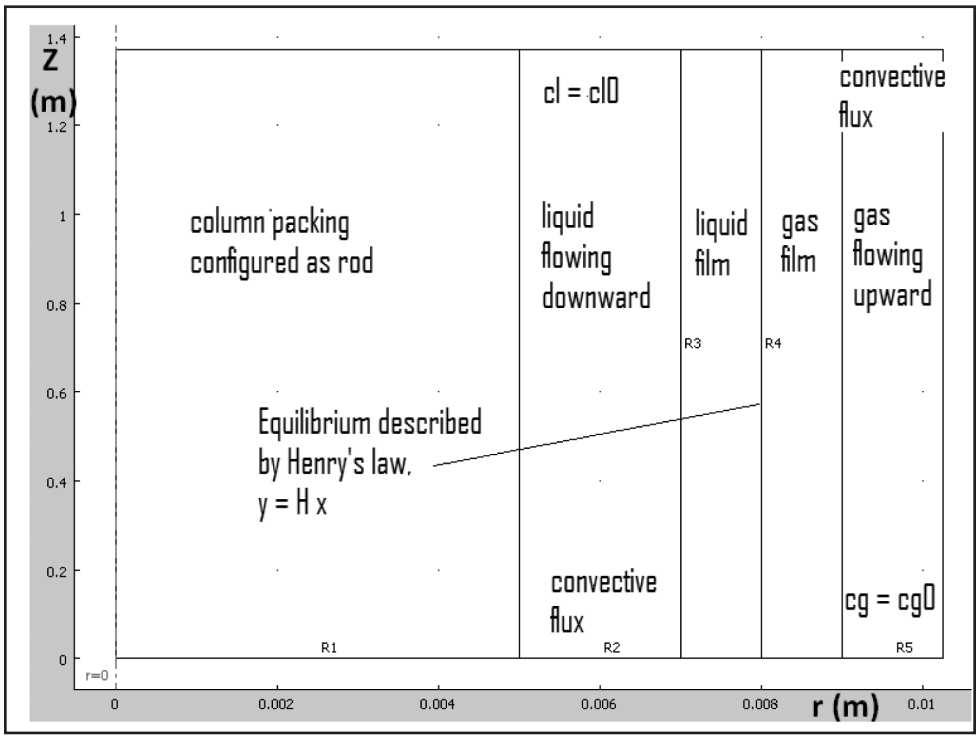

Figure 4. *Model geometry showing two-film theory.*

The mass transfer coefficient was designed to lump all the complexities of the process into a single parameter accounting for the reciprocal of the average resistance to mass transfer throughout the column.[6] As shown above, this approach describes absorption results well, but doesn't give the same insight into the physical process that a diffusion-based model does. To introduce the mass transfer concept into our diffusion-based model we start by comparing diffusion in a complex situation to that of diffusion across a stagnant 1-D film. The steady state flux across a 1-D film is given by Fick's law:

$$\text{Flux} = \frac{D}{l}\Delta c \qquad (13)$$

where l is the film thickness and

Δc is the concentration difference across the film. The mass transfer coefficient was defined to give a similar simple equation for the flux for more complex situations:

$$\text{Flux} = k_c \Delta c \tag{14}$$

One way to understand what the mass transfer coefficient represents is to compare Eqs. (13) and (14) and let

$$k_c = \frac{D}{\delta} \tag{15}$$

where δ is some equivalent stagnant film (or concentration boundary layer) thickness that can be viewed as controlling (providing resistance to) the mass transfer in a complex situation. Note that k_c has units of m/s.

To introduce the two-film concept into our diffusion-based model we could incorporate a stagnant film (with v_g or $v_l = 0$) of the appropriate thickness on each side of the interface and use Eq. (4) (with R = 0 and D = D_g or D_l) over those films. Alternatively, and equivalently, we have used an effective diffusivity acting over an arbitrarily established film thickness, t_{film}, instead of the actual diffusivity over a film thickness, δ, that would need to be adjusted to fit each data point:

$$\frac{D}{\delta} = \frac{D_{eff}}{t_{film}} \tag{16}$$

Figure 4 shows the geometry and boundary conditions for our two-film model based on this effective diffusivity approach. The appropriate resistance to mass transfer in each film has been established by setting the effective diffusivity in the r-direction of the film to be equal to the individual mass transfer coefficient times the film thickness. Obtaining appropriate values for the effective diffusivities requires estimating values of the individual mass transfer coefficients, $k_y a$ and $k_x a$, accounting for the interfacial area per volume, a, as a separate component of $k_y a$ and $k_x a$, and some unit conversions.

From Table 3 it can be observed that $1/k_y a$ is a minor contributor to $1/K_y a$ in Eq. (3), for this system. We have, therefore, chosen to assume that the correlated values of $k_y a$ shown in Table 3 are correct, knowing that uncertainties in these values will not have a strong effect on our subsequent results and interpretations. With this assumption, $k_x a$ could be calculated from Eq. (3) using the previously obtained experimentally derived values of $K_y a$ at each liquid flow rate. The resulting values for $k_x a$ are given in Table 4 (next page). For our model, the interfacial area per volume is $2\pi R_i Z N_R / V = 667\ m^2/m^3$. R_i is the radius of the model at the interface and N_R is the number of glass rods. Taking into account unit conversions between c_g and y and c_l and x yields the following equations for effective diffusivities in the gas and liquid films.

$$D_{g_{eff}} = \frac{k_y a\left(t_{film}\right)\left(8.314 m^3 Pa / mol\ K\right)}{a\left(101325 Pa\right)} \tag{17}$$

$$D_{l_{eff}} = \frac{k_x a\left(t_{film}\right)\left(1000 cm^3 / L\right)}{a\left(55.556 mol / L\right)\left(100 cm / m\right)^3} \tag{18}$$

where t_{film} is the thickness of the stagnant gas and liquid films used in the model (arbitrarily set to 0.001 m).

Note that although we have used mass transfer coefficients in defining our effective diffusivities, our two-film model does not use the mass transfer coefficient approach but instead describes mass transfer as governed only by molecular diffusion through stagnant films, equilibrium at the interface, and convection in the flowing layers (assumed to be in plug flow). We have also artificially increased the diffusivities in the r-direction in the two flowing layers of our model to isolate all the resistance to mass transfer in the stagnant layers. Also note that the value of the interfacial area per volume used here is not necessarily a physically correct value. It is simply the one that matches the arbitrarily chosen flowing layer and film thicknesses and associated number of glass rods of our model.

Solving our explicit two-film model gives the same x and y results as those obtained with our simpler model. In addition, we can observe the concentration at every point in the absorber as shown in Figure 5. By looking at the con-

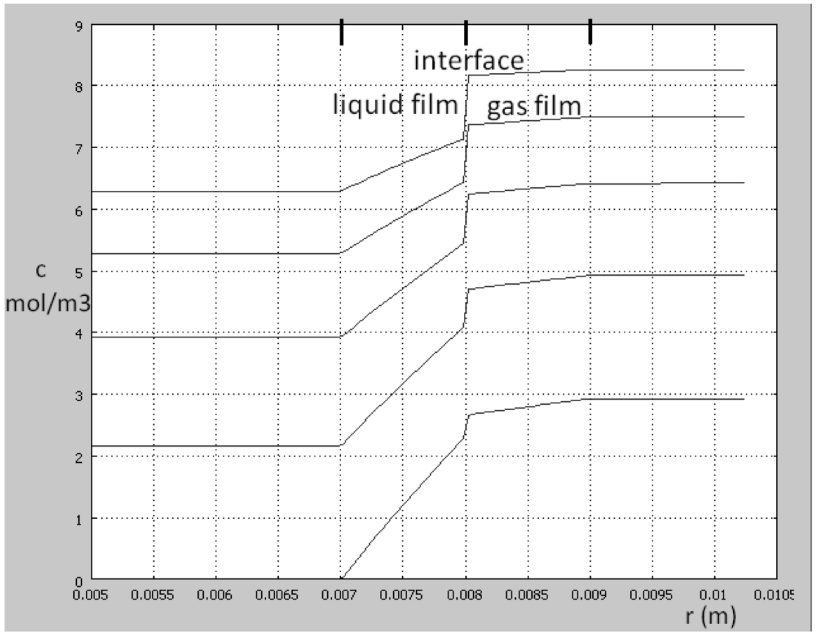

Figure 5. *Concentration in the r-direction for W = 1.58 L/min at various column heights, z/Z = 0, 0.25, 0.5, 0.75, 1.0. Note that the x-axis begins at r = 0.005 m to show only the fluid layers in this figure.*

TABLE 4
Mass Transfer Coefficients and Film Thicknesses
(*adjusted to saturation at liquid outlet).

Water Rate, W L/min	$K_y a$ mol/m^{3}s	H_y m	$k_y a$ mol/m^{3}s	$k_x a$ mol/m^{3}s	k_x mol/m^{2}s	δ_l m $\times 10^5$	δ_g m $\times 10^2$	k_{cl} m/s $\times 10^4$	k_{cg} m/s $\times 10^4$
Large Column	No Reaction								
0.53	0.480*	0.065	3.55	789	1.18	8.45	13.41	0.213	1.19
1.06	0.558	0.046	5.02	891	1.34	7.48	9.49	0.241	1.69
1.58	0.634	0.038	6.13	1004	1.51	6.64	7.77	0.271	2.06
2.11	0.712	0.033	7.08	1123	1.68	5.93	6.73	0.303	2.38
Small Column	No Reaction								
0.14	0.237	0.110	6.53	350	0.525	19.1	7.3	0.095	2.19
0.23	0.285	0.086	8.37	419	0.629	15.9	5.7	0.113	2.81
0.28	0.312	0.078	9.23	458	0.687	14.6	5.1	0.124	3.10
0.35	0.349	0.070	10.32	512	0.768	13.0	4.6	0.138	3.47
0.40	0.375	0.065	11.04	551	0.827	12.1	4.3	0.149	3.71
Small Column	With Reaction								
0.14	2.96	0.110	6.53	7667	11.50	0.870	7.3	2.07	2.19
0.23	3.69	0.086	8.37	9354	14.03	0.713	5.7	2.52	2.81
0.28	4.09	0.078	9.23	10438	15.66	0.639	5.1	2.82	3.10
0.35	4.66	0.070	10.32	12066	18.10	0.552	4.6	3.26	3.47
0.40	5.07	0.065	11.04	13295	19.94	0.501	4.3	3.59	3.71

centration across the various layers at various heights in the column a student can observe the resistance to mass transfer in each of the films as well as the concentration difference imposed by equilibrium at the interface. More resistance is indicated by a larger concentration change. In this system, it can be seen that the liquid phase offers considerably more resistance than the gas phase.

From Table 4 we see that $k_x a$ increases with increasing water rate. This could be due to either k_x increasing or the interfacial area, a, increasing or both. The interfacial area probably does increase with increasing water rate because more of the packing is wetted and the flowing liquid layer may also be thicker. If we assume, however, that a is constant as we have done in our model, we can see that k_x increases with increasing water rate. What physical process can account for this? As shown above, k_c (and with unit conversions k_x) can be assumed to be equal to the molecular diffusivity divided by the stagnant film thickness. Since we used an arbitrary film thickness, t_{film}, for convenience in our model, an estimate of the stagnant liquid film thickness in our absorber can be obtained by solving Eq. (16) for δ_l.

Results for this stagnant film (or concentration boundary layer) thickness estimated by this approach are given in Table 4 at each of the absorbent flow rates studied. Even though the stagnant film thicknesses are fictitious constructs of the film theory and subject to the assumptions in our model, the estimated film thicknesses can be seen to decrease with increasing water rate, thus providing a physical explanation for the observed dependence of mass transfer on water flow rate.

Our explicit two-film model can also be used to provide more insight into the difference between absorption with and without reaction. To include the chemical reaction, we initially used Eq. (7) in the flowing liquid layer only. The resulting concentration profiles at various heights in the small column with and without reaction are shown in Figure 6. For the case with no reaction, in Figure 6a, it can be seen that the liquid side resistance dominates the process. For the reaction case, shown in Figure 6b, the concentration in the flowing liquid is essentially zero everywhere providing a consistently high driving force for mass transfer and preventing saturation of the liquid even at low liquid rates. It can also be seen that the resistance in the gas phase is comparable to the resistance in the liquid phase when reaction is present.

Estimates of the effective film thicknesses in the small column obtained from Eq. (16) are given in Table 4. In accordance with our qualitative falling film model, it can be seen that the chemical reaction has the effect of dramatically reducing the liquid film thickness. The fact that the gas film

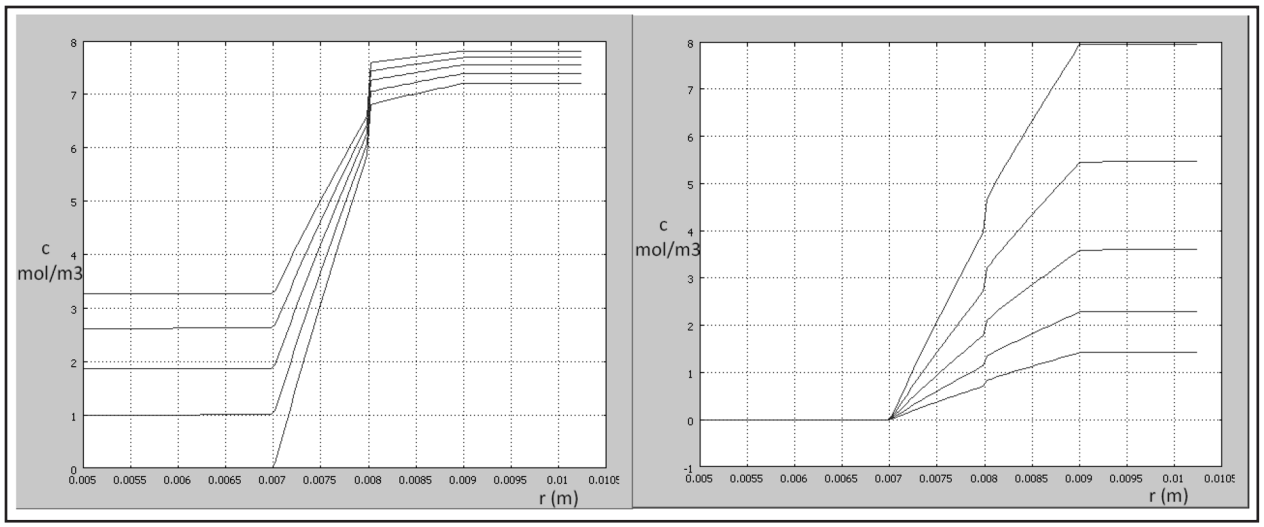

Figure 6. *Concentration profile for W = 0.35 in the small column at z/Z = 0, 0.25, 0.5, 0.75, 1.0: (a) no reaction, (b) with reaction. Note that the x-axis begins at r = 0.005 m to show only the fluid layers in this figure.*

thicknesses are much larger than the liquid film thicknesses can be explained by the fact that the gas phase diffusivity is much larger than that in the liquid phase and does not imply that the gas film offers more resistance than the liquid film. To gain more insight into the resistance offered by each phase it is instructive to compare the k_c values. These values have been calculated from Eq. (15) using film thicknesses reported in Table 4, but it would be equivalent to calculate them from the $k_y a$ and $k_x a$ values using appropriate unit conversions. The resulting values of k_{cl} and k_{cg} shown in Table 4, tell a similar story to the one represented visually in Figure 6. Without reaction, k_{cl} is smaller than k_{cg} indicating that the liquid phase is the controlling resistance. With reaction, the values of k_{cl} and k_{cg} are comparable to one another indicating that the gas phase resistance plays a significant role.

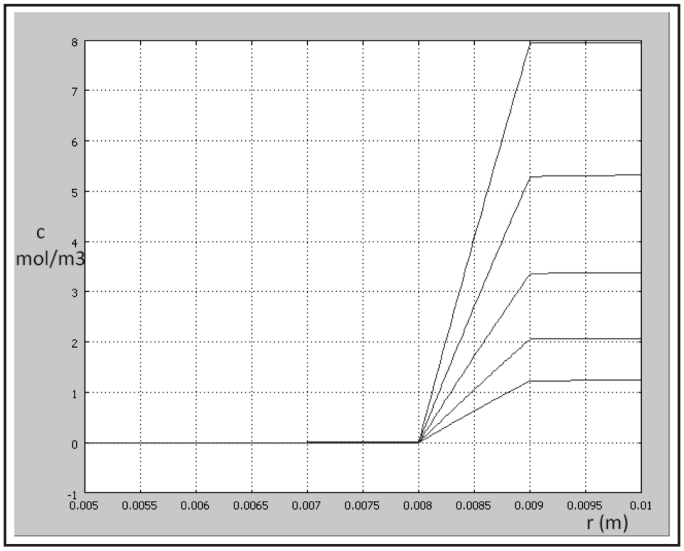

Figure 7. *Concentration profile for W = 0.35 in the small column at z/Z = 0, 0.25, 0.5, 0.75, 1.0 with reaction in the liquid and all mass transfer resistance in the gas film. Note that the x-axis begins at r = 0.005 m to show only the fluid layers in this figure.*

In the analysis above, we considered the stagnant liquid film to account for resistance due to diffusion into the liquid phase separately from the reaction taking place almost instantaneously in the flowing liquid layer. Another way to analyze this type of fast reaction process is to consider that there is no liquid film (or no resistance in the liquid film) since the reaction can take place as soon as the solute crosses the interface. In that case, all the resistance to mass transfer would be in the gas film and the individual gas film mass transfer coefficient would be equal to the overall mass transfer coefficient. We modeled that scenario in our two-film model by setting $k_y a$ equal to the $K_y a$ values shown in Table 3 and setting the effective diffusivity in the r-direction in our liquid film to an artificially large number. The resulting concentration profile shown in Figure 7 gives gas phase concentrations similar to those in Figure 6b. It is possible that Figure 7 is more representative of reality than Figure 6b because the $k_y a$ values used to obtain 6b came from a correlation and are not necessarily correct. Figure 3 obtained from our qualitative model suggests that Figure 6b with a small but extant liquid film might be more realistic than Figure 7, however.

IMPLEMENTATION AND EVALUATION

In our unit operations lab, students spend about two weeks on each experiment. Groups of three or four students first collaborate on writing a pre-lab report describing the relevant theory and their plans to conduct the experiment. For the absorber lab, the groups then spend two days of lab work collecting data that they analyze and include in a final report. It was disappointing, but revealing, that very few students

bothered to use the simulations the first year they were offered as a completely optional resource. In the second offering, we required each student to complete an interactive tutorial containing the simulations and an associated online quiz that asked questions about them. At the end of the course that year, the students completed a survey regarding their perception of the benefits of using the simulations.

Students in the course did not build the simulations from scratch but instead re-ran previously developed simulations with different operating conditions. The tutorial walked the students through the pre-built simulations and included several multiple-choice questions requiring simulation results to obtain correct answers. For example, one question asked for the numerical value of the mole fraction of CO_2 in the exiting liquid stream according to the simulation under certain conditions. Another question asked for the value that would be obtained if the process were considered dilute with straight equilibrium and operating lines. In addition to answering these questions, students were encouraged to experiment with changing operating conditions to see the effect on column performance. Students were invited to study the simulations and answer the multiple choice questions on their own time and at their own pace. They were encouraged to study the simulations before completing their pre-lab reports but were required to submit the answers to the multiple choice questions on-line after the pre-lab was completed and before the final report was due. It should be noted that these students were not necessarily COMSOL model builders but did have some familiarity with COMSOL from previous homework assignments using pre-built simulations via tutorials and online questions.

TABLE 5
Results for Three Survey Questions
The percentage of students giving each response is indicated in brackets.

(1) The learning tool helped me to understand mass transfer, in general: (a) not at all [13%], (b) just a little [13%], (c) somewhat [40%], (d) much [27%], (e) very much [7%].
(2) It helped me understand how the mass transfer coefficient varies with water flow rate: (a) not at all [7%], (b) just a little [7%], (c) somewhat [20%], (d) much [53%], (e) very much [13%].
(3) The best time to use this learning tool would be: (a) as a homework before the pre-lab and in addition to a written pre-lab report [47%], (b) at the pre-lab stage instead of a written pre-lab report [27%], (c) after a written pre-lab and the lab itself are complete, as an aid to writing a good final report [13%], (d) after a written pre-lab and the lab itself are complete, to be used instead of a final report [0%], (e) not necessary for the average student to spend time on this at any point [13%]

TABLE 6
Example Student Comments About the Absorber Simulation

• "it allowed me to visualize the diffusion of gas into the liquid"
• "it allowed me to see the connection between the theoretical equation and how they relate to the physical world"
• "being able to adjust the values and quickly observing changes in the system makes for a nice learning tool"
• "I would not have remembered as much about mass transfer if I didn't have it"
• "really helped me visualize what is occurring and then linking the theoretical values to what is found experimentally, and why it may vary"
• "It allowed me to understand how changing variables could affect the final resistance to mass transfer. By doing this as a simulation, it was easier to see relationships compared to just looking at equations."
• "the ability to change variables and investigate their effects on mass transfer helped provide a greater understanding of mass transfer principles"
• "it basically showed me what the lab would be like … and prepared me for the experiment in an excellent way"
• "It helps you visualize the process and makes it easier for you to make a mistake and rectify it without wasting much time in the lab. And you can also change constants to see the effect of each on mass transfer."

The end of course survey revealed that most, but not all, of the students found the simulations to be useful, particularly for illustrating the resistance to mass transfer and providing a physical feel for why the mass transfer coefficient increases with increasing water rate. Table 5 shows example questions and the percent of students responding to each of the multiple choice answers for each question. Table 6 provides examples of student comments on the absorber simulations.

CONCLUSION

Our new absorption experiment provides an effective way of teaching mass transfer fundamentals while using relatively small amounts of CO_2, air, and water. Experiments presented with NaOH as absorbent provide a good demonstration of the dramatic improvement in absorption due to reaction. A simple model made with COMSOL Multiphysics gives accurate calculations, is easier to use than the traditional analysis, and provides a visual representation of the absorption process. More detailed models that illustrate the concentration boundary layer and the two-film theory provide a physical feel for the observed increase in the mass transfer coefficient with an increase in water rate. These models also make it clear that the improved mass transfer with reaction is due to reduced resistance in the liquid phase as well as maintaining a high driving force and preventing saturation of the liquid. The straightforward and relatively easily obtained solutions together with the richness of information afforded by post processing capabilities in COMSOL can make the details of complex process calculations "come alive" in comparison to the rare, static, printed examples in text books. Combining the experiments with computer simulations that show the concentration profile within the equipment appears to benefit the learning process and help students gain a more complete understanding of mass transfer in an absorber.

ACKNOWLEDGMENTS

This material is based on work supported by the National Science Foundation under grant no. DUE-0536342.

REFERENCES

1. Clark, W.M., and D. DiBiasio, "Computer Simulation of Laboratory Experiments for Enhanced Learning," *Proceedings* of the ASEE Annual Conference, Honolulu, Hawaii, June 24-27, (2007)
2. Clark, W.M., "COMSOL Multiphysics Models for Teaching Chemical Engineering Fundamentals: Absorption Column Models and Illustration of the Two-Film Theory of Mass Transfer," COMSOL Conference 2008 *Proceedings*, Boston, October (2008)
3. Finlayson, B.E., *Introduction to Chemical Engineering Computing*, Wiley-Interscience, Hoboken, NJ, (2006)
4. <http://www.hampden.com>
5. <http://www2.emersonprocess.com/en-US/Pages/Home.aspx>
6. Cussler, E.L., *Diffusion: Mass Transfer in Fluid Systems*, 3rd Ed., Cambridge University Press, New York, (2009)
7. Geankoplis, C.J., *Transport Processes and Separation Process Principles (Includes Unit Operations)*, 4th Ed., Prentice Hall, Upper Saddle River, NJ (2003)
8. Whitman, W.G., "The Two-Film Theory of Gas Absorption," *Che. Metal. Eng.*, **29**, 146-150 (1923)
9. <http://www.comsol.com>
10. Pohorecki, R., and W. Moniuk, "Kinetics of Reaction Between Carbon Dioxide and Hydroxyl Ions in Aqueous Electrolyte Solutions," *Chem. Eng. Sci.*, **43**(7), 1677 (1988)
11. COMSOL Multiphysics, *Chemical Engineering Module User's Guide*, Separation Through Dialysis Example.
12. Seader, J.D., and E.J. Henley, *Separation Process Principles*, 2nd Ed., Wiley, Hoboken, NJ (2006)

APPENDIX

1. Matlab m-files for absorber analysis.

The function quadv is a built-in Matlab function that performs numerical integration of a complex function between finite limits.

```
% run_absorber.m
 % this is the driver file to calculate the overall
gas phase
% mass transfer coefficient, Kya, and the HTU and
NTU for an absorber
% input is Z, packing height (m); S, cross sec-
tional area (m^2);
% L0, liquid flux, (mol/m2s), G0, non absorbing
gas flux (mol/m2s);
% yb, inlet gas mole fraction solute; yt, outlet
gas mole fraction solute.
% inlet liquid is assumed pure solvent
% outlet liquid xb is obtained from mass balance
% ye = ystar = H*x
% Kya is in mol/m^3h
global L0 G0 xb yb yt H
H=1420;
Z = 1.372;
S = 0.00456;
 L0 = 1.06*1000/60/18/S;
G0 = 1.42*1000/(100^3*60*0.022415)/S;
yb = 0.185;
yt = 0.099;
xb = G0/L0*(yb/(1-yb)-yt/(1-yt))/(1+G0/L0*(yb/(1-
yb)-yt/(1-yt)))
NTU = quadv(@funynew,yt,yb)
HTU = Z/NTU
Kya = G0/HTU*3600
% funy.m
% function to integrate to get NTU
function f = funy(y)
global L0 G0 xb yb yt H
OPTIONS=[];
x = G0/L0*(y/(1-y)-yt/(1-yt))/(1+G0/L0*(y/(1-y)-
yt/(1-yt)));
ye=H*x;
f = 1/((1-y)^2*(y-ye));
```

```
>> run_absorber
xb = 1.2597e-004
NTU = 3.3846
HTU = 0.4054
Kya = 2.0563e+003 ❒
```